International Journal of Multiphase Flow 35 (2009) 439–449

Contents lists available at ScienceDirect

International Journal of Multiphase Flow

journal homepage: www.elsevier.com/locate/ijmulflow

A growth model for dynamic slugs in gas–liquid horizontal pipes

U. Kadri *, M.L. Zoeteweij, R.F. Mudde, R.V.A. Oliemans

Department of Multi-Scale Physics, Delft University of Technology, Prins Bernhardlaan 6, 2628 BW, Delft, The Netherlands

ARTICLE INFO

Article history:
Received 16 August 2008
Received in revised form 6 January 2009
Accepted 7 February 2009
Available online 21 February 2009

Keywords:
Long liquid slugs
Gas–liquid pipe flow
Flow regime transition

ABSTRACT

Long liquid slugs, with sizes reaching 500 pipe diameters or more, may form in gas–liquid horizontal pipe flow at intermediate liquid loadings. Such slugs cause serious operational upsets due to the strong fluctuations in flow supply and pressure. Therefore, predicting the transition from short (hydrodynamic) to long slug flow regimes may play a significant role in preventing or reducing the negative effects caused by the long slugs.

In this paper we introduce a growth model for calculating the average slug length in horizontal and near horizontal pipes. The model applies a volumetric balance between the front and tail of the slug in order to calculate the slug growth rate. The dynamic behaviour of the liquid at the tail is described by a linear kinematic relation between the slug downstream and the wave upstream.

For the validation of the model we performed measurements in a 137 m length air–water horizontal pipe flow of an internal diameter (i.d.) of 0.052 m. The measurements provide a detailed flow map of the long slug regime and sub-regimes. Furthermore, we compared predictions by the model with available data for a range of 0.019–0.095 m i.d. pipes to investigate the effect of varying operation pressures, different inlet conditions, different fluid properties and slight inclinations. The model predicted the transitions from hydrodynamic to long slugs with satisfactory agreements, however it underpredicts the average slug length at relatively large mixture velocities.

1. Introduction

Slug flow is commonly observed in horizontal and slightly inclined pipe flows. It is characterized by the appearance of plugs of liquids, moving downstream, separated by elongated bubbles, moving along the top of the pipe. Although mostly short hydrodynamic slugs are observed, at relatively low gas flow rates very long slugs with sizes reaching 500 pipe diameters or more may form. Such long slugs cause severe operational failures due to the strong fluctuations in flow supply and pressure. A frequent appearance of the long slugs is likely to occur in older gas production offshore fields, where the operation pressure is low. Therefore, predicting the transition from regular hydrodynamic to long slug regimes plays a prominent role in preventing or reducing future operational failures.

Two theoretical concepts are used to predict the flow conditions at which, both hydrodynamic and long, slugs are observed: stability of stratified flow and stability of slugs. The stability of stratified flow describes waves on thin films over which gas is blowing (Hanratty and Hershman, 1961). Whereas slug stability analysis considers a volumetric liquid balance between the front and the tail of a slug. For a fully developed slug moving at the bubble velocity, this balance results in the minimum liquid height, $h_{L_{min}}$, at the front required for the slug to be stable (Ruder et al., 1989; Bendiksen, 1984). Measurements and photographs done by Woods and Hanratty (1996) support the idea that the back of a slug can be modelled as a bubble (Benjamin, 1968). Hurlburt and Hanratty (2002) compared predictions by slug stability for the critical superficial liquid velocity, $U_{SL_{crit}}$, needed for transition to slug flow, with transition measurements by Andritsos et al. (1989). The comparisons show that the theoretical predictions of $U_{SL_{crit}}$ overpredict measurements with a factor of two. The overprediction reflects inaccuracies in estimating the interfacial shear stresses (Hurlburt and Hanratty, 2002).

Wallis and Dobbins (1973), Lin and Hanratty (1986) and Wu et al. (1987) followed the analysis by Hanratty and Hershman (1961) to examine the growth of a viscous long wavelength instability (VLW). The VLW theory correctly predicts that the critical gas velocity needed for the transition from stratified to slug flow for air–water flows will increase with increasing pipe diameter; however, it predicts very different effects of liquid viscosity (Hurlburt and Hanratty, 2002). On the other hand, Kristiansen (2004) made an experimental investigation based on slug and stratified inlet conditions and found different critical liquid height, $h_{L_{crit}}$, and $U_{SL_{crit}}$ for the two different flow inlet cases. He found that $h_{L_{crit}}$ and $U_{SL_{crit}}$ are successfully predicted by slug stability model for slug flow inlet conditions, whereas $h_{L_{crit}}$, is well predicted by VLW for stratified flow inlet conditions only at low gas flow rates. On the basis of these findings, Kadri et al. (2008) presented a new model

* Corresponding author. Tel.: +31 27 83210; fax: +31 27 82838.
E-mail address: U.Kadri@tudelft.nl (U. Kadri).

0301-9322/$ - see front matter © 2009 Elsevier Ltd. All rights reserved.
doi:10.1016/j.ijmultiphaseflow.2009.02.003

for predicting the average slug length as a function of time. The model applies a volumetric balance between the front and tail of a slug in order to calculate the slug growth rate and length. At the front, VLW was used to calculate the liquid height, $h_{L_{VLW}}$; and at the tail linear kinematic relations and geometric considerations were used to describe the dynamic behaviour of the liquid at the slug tail. Kadri et al. (2008) postulated that the slug tail extends due to the fact that the back of the slug travels faster (at the bubble velocity) than the tail upstream, which they assumed to travel at the wave velocity. In their model, the slug reaches its final length when the ratio between the length of the extended slug tail to the calculated slug length equals the ratio between the bubble to the slug average lengths. The ratio of the latter is based on conservation of mass were the average liquid height in bubbles of the fully developed slug flow is calculated from slug stability ($h_{L_{min}}$). Their model is only valid at low U_{SG} when $h_{L_{VLW}} > h_{L_{min}}$.

In this paper we extend the work by Kadri et al. (2008) such that larger ranges of flow rates can be applied. Here, we considered the average maximum liquid height, $h_{L_{max}}$, that can appear at the slug front instead of $h_{L_{VLW}}$ (when $h_{L_{VLW}} < h_{L_{min}}$). The parameter $h_{L_{max}}$ is, therefore, the equilibrium level of the liquid phase for the given flow conditions assuming stratified flow. Special attention was given for predicting the transition from hydrodynamic to long liquid slugs. For the validation of the model we performed slug length measurements in a 137 m long air–water horizontal pipe flow of an internal diameter (i.d.) of 0.052 m. The measurements are original and unique in the sense that they provide a clear and detailed presentation of the long slug regime which is, unlike the hydrodynamic slug regime, not well reported in the literature. Moreover, we compare theoretical predictions of the model with measurements done by Kristiansen (2004) for 0.06 and 0.069 m i.d. pipes at different, flow rates, operation pressures, fluids properties, and slight inclinations. We also compare theoretical predictions with slug length calculations based on frequency measurements by Gregory and Scott (1969), Hubbard (1965), Woods and Hanratty (1999) and Fan et al. (1993) for 0.01905, 0.0351, 0.0763 and 0.095 m i.d. pipes, respectively. The predictions show a satisfactory agreement with the slug length measurements, and a qualitative agreement with the slug length calculations (from slug frequency measurements).

Theoretical background including stability of stratified flow, VLW and slug stability is presented in Section 2. The experimental setup and the methods used for performing the measurements are given in Section 3. In Section 3 we further present an overview of the regimes in the flow map and sub-regimes in the slug flow regime, as found in the experiments. Section 4 provides a detailed analysis of the proposed model for calculating the final average slug length. Comparisons between theory and measurements are given in Section 5. Finally, a discussion and the conclusions are presented in Section 6.

2. Theoretical background

2.1. Stratified flow pattern

An idealized model of the stratified flow pattern is represented by a simplified geometry as given in Fig. 1. The diameter of the pipe is D. The height of the liquid layer along the centerline is h_L. The length of the segments of the pipe circumference in contact with the gas and liquid are S_G and S_L, respectively. The length of the gas–water interface is represented by S_i. The areas occupied by the gas and the liquid are A_G and A_L, respectively. Given the pipe diameter and the liquid height (or area), these parameters can be calculated using the geometric formulae by Govier and Aziz (1972). Now we can write the momentum balances for the gas and the liquid flows as follows:

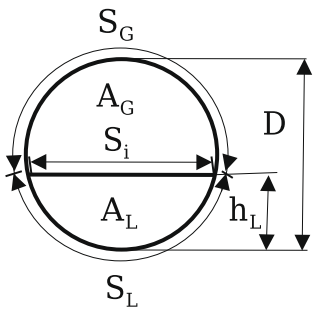

Fig. 1. Cross-section of the pipe, stratified flow representation.

$$-A_G\left(\frac{dP}{dx}\right) - \tau_{WG}S_G - \tau_i S_i + \rho_G A_G g \sin\theta = 0, \quad (1)$$

$$-A_L\left(\frac{dP}{dx}\right) - \rho_L g \cos\theta\left(\frac{dh_L}{dx}\right) - \tau_{WL}S_L + \tau_i S_i + \rho_L A_L g \sin\theta = 0 \quad (2)$$

where ρ_G and ρ_L are the gas and the liquid densities, θ is the inclination angle of the pipe from the horizontal, dp/dx is the pressure gradient, dh_L/dx is the liquid hydraulic gradient, and g is the acceleration due to gravitational forces. The time-averaged resisting stress of the gas and the liquid at the wall are τ_{WG} and τ_{WL}, respectively. Term τ_i represents the resisting stress at the interface. The stresses τ_{WG}, τ_{WL} and τ_i are defined in terms of friction factors, which are calculated using the Blasius equation if $Re < 10^5$ and the wall roughness effect can be ignored, otherwise the Churchill equation is used (see Churchill, 1977). For given flow rates of the gas and the liquid, Eqs. (1) and (2) are used to find the pressure gradient and the height of the liquid layer. However, these equations do not determine the stability of the stratified flow. The flow is assumed to be varying slowly enough that pseudo-steady-state assumptions can be made (e.g. $dh_L/dx = 0$ and τ_{WG}, τ_{WL} and τ_i can be related to flow variables).

2.2. Viscous long wavelength theory

The transportation of gas and liquid in horizontal pipes results in a wide range of wavelength waves and wave frequencies along the pipe. At low gas and liquid flow rates, high frequency waves are formed close to the inlet (Woods and Hanratty, 1999). Among those, waves with frequencies 10–12 Hz grow and bifurcate further downstream due to energy accumulations (Fan et al., 1993). The bifurcation results, among other, in long wavelength waves that can grow, roll or decay, depending on the height of the liquid layer (Fan et al., 1993). For the "right" flow conditions, they grow to become slugs. If the pipe is long enough and the long wavelength waves form far downstream the inlet such that the evolving slugs are independent from the flow disturbances at the inlet, the slugs can grow to become extremely large.

The viscous long wavelength (VLW) stability theory describes such long waves on thin films over which gas is blowing. The waves are assumed to be long enough so that a change in pressure can be described by a hydrostatic approximation and the stresses vary so slowly in time that a pseudo steady-state approximation describes the change in stresses. The equations of conservation of mass and momentum for the liquid phase in the horizontal pipe are, respectively,

$$\frac{\partial A_L}{\partial t} + \frac{\partial (uA_L)}{\partial x} = 0, \quad (3)$$

and

$$\frac{\partial(uA_L)}{\partial t}+\frac{\partial(u^2A_L)}{\partial x}=-\frac{A_L}{\rho_L}\left(\frac{\partial P}{\partial x}+\rho_L g\cos\theta\frac{\partial h_L}{\partial x}\right)+\frac{1}{\rho_L}(\tau_i S_i-\tau_{WL}S_L)+A_L g\sin\theta, \quad (4)$$

A disturbance is assumed to occur at the interface,

$$A_L=\overline{A}_L+\hat{A}_L exp[ik(x-Ct)], \quad (5)$$

where $\overline{A}_L$ is the average area occupied by the liquid, $\hat{A}_L$ is the amplitude of the disturbance, C is the complex wave velocity and k is the wave number.

Introducing complex amplitudes of the wave-induced variations of the pressure and of the resisting stresses and substituting equations of the form of Eq. (5), Lin and Hanratty (1986) obtained a relation for the critical velocities for the initiation of a long wavelength disturbance,

$$0=\rho_L(C_R-\bar{u})^2+\frac{\overline{A}_L}{\overline{A}_G}\rho_G(\overline{U}-C_R)^2-g\overline{A}_L\rho_L cos\theta\frac{\hat{h}}{\hat{A}_L}. \quad (6)$$

Terms $\overline{U}$ and $\bar{u}$ are the time average gas and liquid velocities. Term C_R is the real part of C, for given superficial gas and liquid velocities at neutral stability, where C_I, the imaginary part of C, is zero. Substituting the critical velocities in Eq. (4) results in the liquid area, $A_{L_{VLW}}$ (or $h_{L_{VLW}}$), required for the initiation of instabilities at the surface (e.g. waves or slugs). A detailed analysis of the VLW theory can be found in Lin and Hanratty (1986) and in Hurlburt and Hanratty (2002).

2.3. Slug stability analysis

The slug stability analysis considers the rates of liquid adjoining and detaching from a slug at its front and rear. Slugs are defined here as stable when the rates of liquid adjoining are not less than the rates at which liquid detaches, and they are addressed as "neutrally stable" when their length is neither growing nor decaying. Fig. 2 gives an illustration of a slug moving with a front velocity C_F over a stratified liquid layer, at station 1, of area A_{L1} and velocity u_1. The volumetric flow rate of liquid adjoining the slug is

$$Q_{in}=(C_F-u_1)A_{L1}. \quad (7)$$

The rear of the slug is assumed to behave as a bubble moving with a velocity C_B. Following Bendiksen (1984), Woods and Hanratty (1996), Hurlburt and Hanratty (2002) and Soleimani and Hanratty (2003) the velocity at the back of a slug can be modelled as a Benjamin bubble (Benjamin, 1968) where three main regimes are defined:

$$C_B=U_{Mix}+0.542\sqrt{gD}, \qquad U_{Mix}<2\sqrt{gD}, \quad (8)$$

$$C_B=1.1U_{Mix}+0.542\sqrt{gD}, \qquad 2\sqrt{gD}<U_{Mix}<3.5\sqrt{gD}, \quad (9)$$

$$C_B=1.2U_{Mix}, \qquad U_{Mix}>3.5\sqrt{gD}. \quad (10)$$

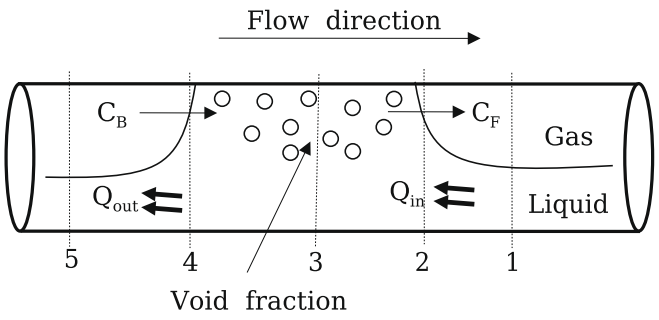

Fig. 2. Sketch of a slug (after Woods and Hanratty, 1996).

The velocity of the liquid in the slug is u_3 (the liquid velocity at station 3). The volume fraction of the gas in the slug is ϵ. The volumetric flow rate of the liquid detaching from the slug is

$$Q_{out}=(C_B-u_3)(1-\epsilon)A, \qquad \text{at section 3.} \quad (11)$$

Assuming neutral stability, $Q_{in}=Q_{out}$ and $C_F=C_B$, and making use of Eqs. (7)–(11), the following relation is obtained,

$$\left(\frac{A_{L_1}}{A}\right)_{crit}=\frac{(C_B-u_3)(1-\epsilon)}{(C_B-u_1)}, \quad (12)$$

for the area of the stratified flow. For incompressible flow, the term u_3 is calculated from a volumetric balance between the inlet of the pipe and station 3 as follows:

$$U_{Mix}=\epsilon U_3+(1-\epsilon)u_3, \quad (13)$$

where U_3 is the gas velocity at station 3. At low mixture velocities aeration is negligible ($\epsilon=0$) so that Eq. (13) gives $u_3=U_{Mix}$. Eq. (12) is used later to calculate the average liquid level below the elongated bubbles in the "fully developed" slug flow. The detailed analysis of the slug stability model is well documented by Hurlburt and Hanratty (2002) and Soleimani and Hanratty (2003).

3. Experiments on the occurrence of long slugs

3.1. Experiments

Experiments have been carried out in order to investigate the long slug regime (Zoeteweij, 2007). Not many researchers are aware of this regime and its properties due to a number of conditions required for such slugs to appear, e.g. long pipe and low flow rates and operation pressure. The flow facility used for this aim consists of a 137 m long horizontal pipeline with a diameter of 0.052 m (see Fig. 3). The pipe is made of perspex (Plexiglas) to allow visual observations of the flow conditions. At the inlet, the two phases are combined in a Y-shaped section with the gas phase always entering from the top in a horizontal direction in order to prevent the impact of the gas-jet coming from above. The pressure is atmospheric and the gas and liquid phases used are air and water, respectively.

Two different measurement techniques, based on liquid conductance, were installed. The first consists of point detector sections positioned at 8 locations along the pipe at: 29, 43, 62, 74, 93, 107, 120, and 132 m from the inlet. A schematic drawing of these positions is given in Fig. 4. Each measurement section contains 2 pairs of sensors separated by 70 cm. Each pair of sensors consists of two electrodes one at the bottom of the pipe and the second on top. Due to the fact that the electrodes at the bottom are circular plates of 1 cm diameter the electrical conductance between the liquid phase and the electrodes are always good. The slug length and velocity are calculated from the time difference of the slug passing two different sensors of the same section: (1) the velocity is calculated from the distance between the two sensors divided by the time difference; and (2) the slug length is calculated from the velocity and the time difference between the front and tail passing the same sensor. The second measurement technique is based on wire-mesh sensors. Unlike the point probe sensors, this technique provides a detailed flow imaging in stratified and slug flows. The technique is based on the difference in electrical conductivity of both phases. A set of 4 sensors is used at different positions: 38, 56, 105 and 125 m from the inlet (see Fig. 4). Each sensor consists of two planes with 16 parallel 0.12 mm wires each. The wires in different planes are perpendicular to each other. Measuring the signal of all vertical receiver wires crossing a horizontal sending one results in the local conductivity around the crossing points in the mesh. The conductivity signals

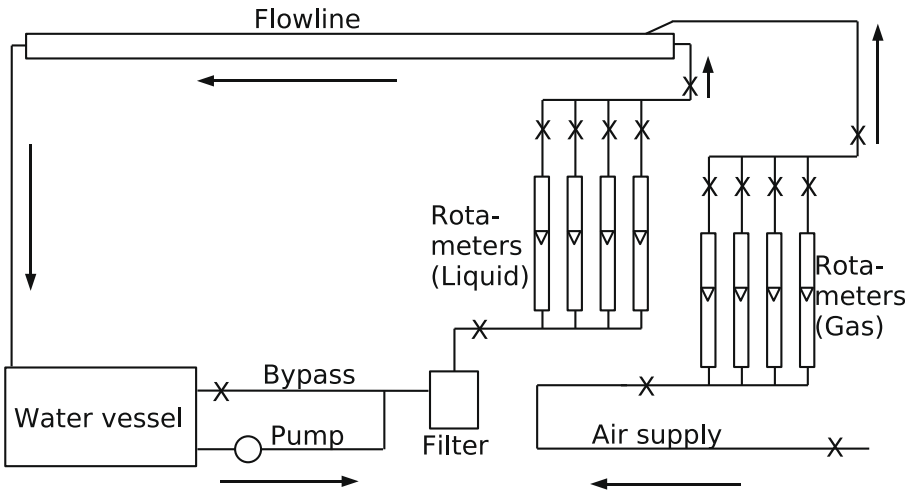

Fig. 3. Sketch of the experimental setup (after Zoeteweij, 2007). The valves are indicated by ×.

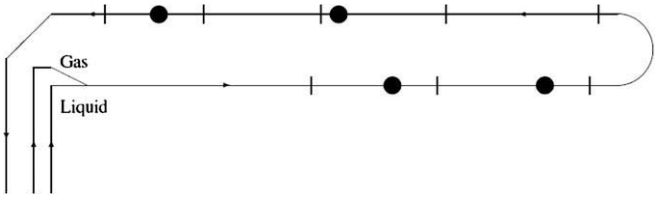

Fig. 4. Schematic drawing of the position of the point probe (|) and wire-mesh (●) sensors (after Zoeteweij, 2007).

indicate the local phase composition in the grid cell. Further details on the wire-mesh can be found in Zoeteweij (2007).

The experiments were performed at atmospheric pressure and constant flow rates with superficial gas and liquid velocities being 0.5–2.5 and 0.05–0.30 m/s, respectively. The different combinations of flow rates used in the experiments resulted in a detailed overview of the slug flow development in different regimes, and sub-regimes within the long slug flow regime.

3.2. Sub-regimes in the slug flow map

The different flow regimes and a number of different sub-regimes within the long slug flow regime observed in the experiments are shown in Fig. 5. The dashed–dotted line is the observed transition from stratified (×) or stratified-wavy flow (∗) to slug flow; the solid-line is the observed transition from hydrodynamic slug flow (○) to the long slug flow regime. Within the long slug flow regime, two sub-regimes were observed: (1) above the dashed-line long but neutrally stable slugs (▲); and (2) below the dashed line, long and positively growing slugs were found (●).

The hydrodynamic slugs are characterized by a relatively short length, less than 40*D*. Whereas the long slugs have at least a length of 40*D* and can reach lengths up to several hundred pipe diameters. Note that the long slug region shrinks for increasing gas velocity – the long slugs are found to exist only at low gas and liquid flow rates, as shown in Fig. 5. Therefore, the transition from stratified flow to hydrodynamic slugs, at low superficial gas velocities, passes through the long slug regime. For higher superficial gas velocities, $U_{SG} > 2.5$ m/s, the transition from the stratified-wavy to hydrodynamic slug flow is direct. The absence of the long slugs at higher U_{SG} is related to the higher slug frequency and lower amount of liquid adjoining the passing slug due to a decrease of the liquid level (conservation of mass and momentum) which results in a neutral stability ($Q_{in} = Q_{out}$ and $C_F = C_B$) earlier in the pipe. Consequently, in the long slug regime, the slug length and growth time decrease at larger flow rates, as observed in the experiments.

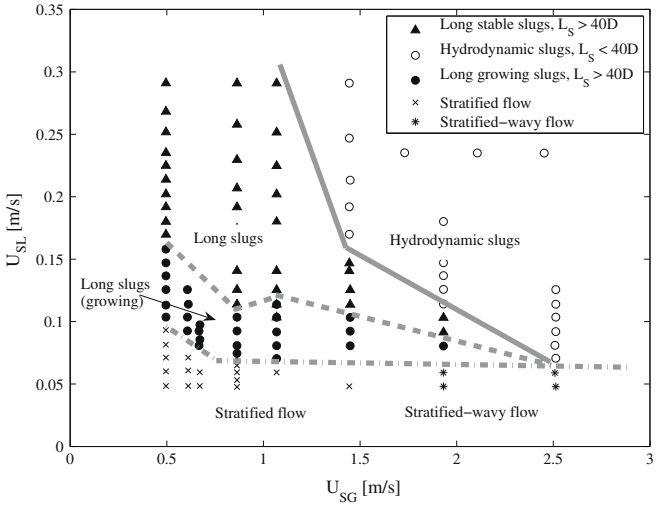

Fig. 5. Air–water measurements of the slug flow regime and sub-regimes for different U_{SG} and $U_{SL}, D = 5.2$ cm, $\theta = 0^\circ, P = 1$ bara.

Fig. 6 is a flow regime map by Woods and Hanratty (1999) for air–water flow in horizontal 0.0763 m pipe. In the figure, curve *A* indicates the transition from stratified to slug flow; the region between curves *A* and *B* (areas *I* and *II*) covers slugs that form about 40*D* downstream of the entrance; area *III* represents slugs that form within 40*D* from the entrance; and along curve *C* the Froude number, $Fr = u/\sqrt{gh_{Lmax}}$, is unity at the inlet. Comparing Figs. 5 and 6, and noting the difference in the diameters, we find the following: (1) the long growing slugs correspond to the slugs evolving from long wavelength waves downstream (at $Fr < 1$). (2) The long stable slugs evolve from the same type of waves but further upstream. Their frequency is higher and they travel over a thinner liquid layer, that is why they reach neutral stability earlier in the pipe. (3) The hydrodynamic slugs correspond to slugs that form upstream (close to the inlet) at $Fr > 1$. These slugs are no longer formed by the long wavelengths but close to the entrance by disturbances that are created there (Woods and Hanratty, 1999). The high frequency of such slugs and the thin liquid layer

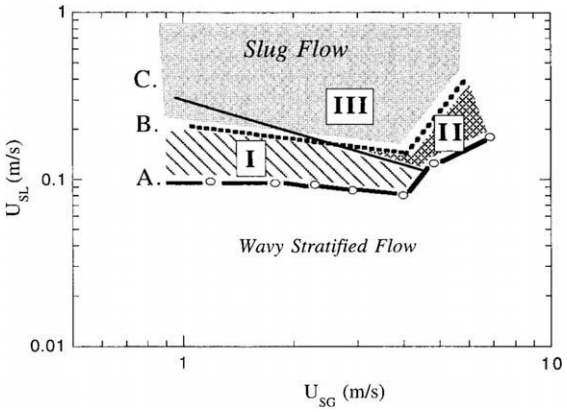

Fig. 6. Flow regime map for air–water flow in horizontal 0.0763 m pipe. Curve *A* indicates the transition to slug flow; between curves *A* and *B*, slugs from downstream ca. 40*D*; along curve *C*, Froude number $Fr = 1$ at the inlet (Woods and Hanratty, 1999). Reprinted from International Journal of Multiphase Flow, vol. 25, Bennett D. Woods, Thomas J. Hanratty, Influence of Froude number on physical processes determining frequency of slugging in horizontal gas–liquid flows, 1195–1223, Copyright (1999), with permission from Elsevier.

downstream result in their short length. These findings are in agreement with our above mentioned experimental observations.

4. Dynamic slug model

In the model presented here, the average length of a fully developed slug is determined from volumetric liquid considerations between the front and the tail of a slug. The liquid level at the front is assumed to be constant, whereas at the back, the liquid level drops during the initiation of the slug and then rebuilds during its growth. The liquid level at the back is obtained from linear kinematic relations between the slug and the wave behind it. The properties of slugs at formation time are presented in Section 4.1. In Section 4.2, the calculation method of the dynamic slug is introduced. A stopping criterion for the calculation of the slug growth, based on conservation of mass of the gas and liquid phases, is addressed in Section 4.3.

4.1. Properties of forming slugs

4.1.1. Wave velocity

We address the formation of slugs from growing waves. The growing waves are assumed to be sinusoidal with an initial wavelength, λ, large compared to the average maximum liquid height, $h_{L_{max}}$. A characteristic property of such waves is the dependency of the wave velocity, *C*, on the liquid level alone,

$$C = \sqrt{g h_{L_{max}}}. \tag{14}$$

4.1.2. Slug at initiation

When a wave keeps on growing, its amplitude will eventually be so large that the top of the wave hits the top of the pipe. This is the initiation of a slug. As the initiated slug is the result of a growing wave, its initial shape will be sinusoidal (note that after the initiation the slug grows and changes shape and it is no longer sinusoidal). Here, the front of the wave is addressed as *slug-wave*, and the back as *tail-wave*. These two parts of the wave are coupled via a mass balance; the liquid required to create the slug is shed from the tail-wave. The amplitude of the front of the wave (slug-wave) is

$$\eta_c = D - h_{L_{max}}, \qquad 0 < h_{L_{max}} < D, \tag{15}$$

as the wave started from the stratified layer of height $h_{L_{max}}$. At the back of the wave (tail-wave), the amplitude η_t will be the same, provided that $\eta_c \leqslant h_{L_{max}}$. Otherwise, the amplitude of the tail-wave is

$$\eta_t = h_{L_{max}}, \qquad h_{L_{max}} \leqslant D/2. \tag{16}$$

In this case, the length of the tail-wave, $\lambda_t/2$, is no longer equal to the length of the slug–tail $\lambda_c/2$ (which is $\lambda/2$). The actual length of the tail-wave in this case is computed from a simple mass balance (i.e. all extra liquid in the slug-wave comes from liquid originally filling up the tail-wave) and the pipe geometry at the location of the tail-wave. The length of the tail-wave is then calculated using the geometric formulae by Govier and Aziz (1972). A schematic drawing of a slug at initiation is given in Fig. 7. In the figure, the parameters A_{L5} and u_5 are the liquid area and velocity at the trough (station 5). The term $A_{L_{min}}$ is the critical liquid area calculated by the slug stability model (Eq. (12)). The hatched area, $A_{G,trough}$ is the gas area between $A_{L_{min}}$ and A_{L5}.

4.1.3. Slug tail extension

At slug formation time, t_0, the slug front and the back of the tail-wave, at point *c*, propagate at the actual velocities C_F and *C*, respectively. On the other hand, the back of the slug propagates at the bubble velocity C_B. The front of the tail-wave (point *O*) is obviously the back of the slug. Therefore, it propagates together with the back of the slug. The $A_{L_{min}}$ line in Fig. 7 is the slug stability line representing the average liquid level below the bubbles in the fully developed slug flow. Points *a* and *b* refer to two points on the tail-wave (at time t_0) being at the height of the final liquid level, $h_{L_{min}}$ (calculated from $A_{L_{min}}$).

Due to the relative velocity between the two sides of the tail-wave (points *O* and *c*) the wave volume in between is expanded in time. While point *a* propagates with the slug back at velocity C_B, from a linear expansion point *b* propagates at a velocity,

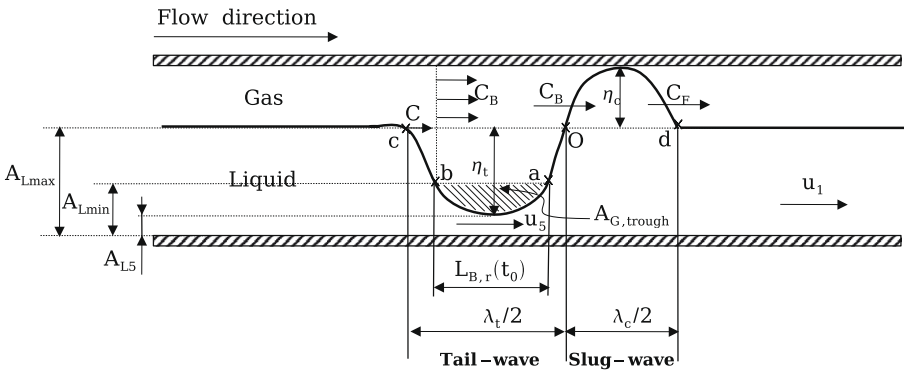

Fig. 7. A slug at initiation time expressed as two sinusoidal waves.

$$v_b = C + r(C_B - C), \tag{17}$$

where r is the ratio between the horizontal displacements of points b, calculated from the wave equation, and a relative to c. The ratio r has a value $0 \leqslant r \leqslant 1$. Due to the relative velocity between points a and b the relative distance between them, $L_{B,r}$, grows linearly as

$$L_{B,r}(t) = L_{B,r}(t_0) + v_b t. \tag{18}$$

Eq. (18) describes the extension of the tail in time. It plays a major role in a stopping criterion for the calculations of the average slug length, as will be seen in Section 4.3.

4.1.4. Initial slug length

The initial slug length, L_0, is calculated from the wavelength, λ,

$$L_0 = \frac{\lambda}{2}. \tag{19}$$

Term λ is calculated from the wave velocity ($\lambda = C/f_w$) and the relation $f_w = c_w f_s$ by Tronconi (1990) for the slug and the wave frequencies, f_s and f_w, as follows:

$$\lambda = \frac{C}{c_w f_s}, \tag{20}$$

where c_w is a constant equal to 2 for air–water systems (Tronconi, 1990). In this paper the same value of c_w was used for the different fluids. Kadri et al. (2008) suggested to use a correlation by Nydal (1991) for the slug frequency,

$$f_s = 0.088\frac{(U_{SL} + 1.5)^2}{gD}. \tag{21}$$

Quantities in Eq. (21) are in meters and seconds. The application condition of Eq. (21) is that the frequency of slugs is dominated by U_{SL}. Note that the slug frequency correlation is used here only in order to obtain a "realistic" initial length of the long waves (which are in agreement with experiments). Other methods can be implemented to obtain an initial wavelength. Alternatively, L_0 can be calculated from the minimum stable slug length by Dukler et al. (1985).

4.2. Slug growth and final length

The calculations of the slug growth are not sensitive to small changes in the initial wavelengths especially for long slugs where the final length of slugs $L_{S,f} \gg \lambda$. Therefore, the main contribution to the final slug length is the additional slug growth due to the volumetric differences between liquid adjoining the slug at the front and detaching from the slug at the trough. The volume of the liquid in front of the slug is the product of the cross-sectional area, $A_{L_{max}}$, occupied by the liquid times the length of this liquid part. Similarly, for the liquid volume at the back of the slug, we need to calculate the cross-sectional area of the liquid layer at the trough. Hence, we need to calculate the two liquid areas, at the trough and downstream the slug.

4.2.1. The liquid area downstream the slug, $A_{L_{max}}$

The liquid area downstream is calculated from the momentum balances for the stratified flow pattern, Eqs. (1) and (2). Substituting $A_L = A_{L_{max}}$ and $A_G = A - A_{L_{max}}$, Eq. (1) is written in the following form:

$$\left(\frac{dP}{dx}\right) = \frac{\tau_{WG}S_G - \tau_i S_i}{A - A_{L_{max}}} + \rho_G g \sin\theta. \tag{22}$$

Plain stratified flow is reached when the pressure gradients of the two phases on the interface cancel each other. Therefore, substituting Eq. (22) in Eq. (2) and after basic algebra we obtain,

$$A_{L_{max}} = A\frac{\tau_{WL}S_L - \tau_i S_i}{\tau_{WL}S_L + \tau_{WG}S_G} + g(A - A_{L_{max}})\left[\rho_L \cos\theta\left(\frac{dh_L}{dx}\right) - A_{L_{max}}\sin\theta(\rho_L - \rho_G)\right]. \tag{23}$$

For a fully developed horizontal flow Eq. (23) reduces to the simple form,

$$A_{Lmax} = A\frac{\tau_{WL}S_L - \tau_i S_i}{\tau_{WL}S_L + \tau_{WG}S_G}. \tag{24}$$

Eq. (24) successfully predicts that increasing the gas flow rates or decreasing the liquid flow rates results in a lower $A_{L_{max}}$.

At low flow rates slugs evolve downstream from long wavelength waves as mentioned above. In that case, the liquid level of the stratified flow at t_0 is calculated by VLW theory. If the liquid flow rates are larger than those predicted by VLW theory, we use Eq. (24) for the calculation of the stratified liquid level. On the other hand, the minimum liquid area, $A_{L_{min}}$, at the front of a fully developed slug is calculated by the slug stability model, Eq. (12), as mentioned earlier.

4.2.2. The liquid area upstream the slug, $A_{L5}(t)$

Making use of the neutral stability assumptions ($Q_{in} = Q_{out}$ and $C_F = C_B$), the liquid velocity at the trough u_5 is obtained from a volumetric flow balance between the liquid entering at station 1 (front) and detaching at station 5 (see Fig. 2) for the fully developed case, thus

$$u_5 = u_1\frac{A_{L_{min}}}{A_{L5}(t)}, \tag{25}$$

where u_1 is the liquid velocity downstream the slug (station 1) and $A_{L5}(t)$ is the cross-section area of the liquid at the trough.

The average velocity of the gas above $A_{G,trough}$ is assumed to be the bubble velocity C_B and therefore the gas volume is conserved there. This also implies that the initial gas volume above the trough and below $A_{L_{min}}$ is constant (see the hatched area in Fig. 7). Since $h \ll \lambda$ the area $A_{G,trough}$ was considered instead of the volume. The parameter $A_{G,trough}$ is calculated by integrating the wave function between points a and b at any time t as follows:

$$A_{G,trough} = \left[h_{L_{min}} - h_{L5}(t)\right]\int_b^a sin\left[\frac{2\pi}{\lambda_c + 2(C_B - C)t}x\right]dx. \tag{26}$$

The left-hand side of Eq. (26) is a constant. Therefore, substituting two cases in Eq. (26), the first $t = 0$ and the other $t = t$, and equating between them results in the liquid level at the trough, $h_{L5}(t)$, as follows:

$$h_{L5}(t) = h_{L_{min}}\left[1 - \frac{\lambda_c}{\lambda_c + 2(C_B - c)t}\right] + h_{L5}(0)\frac{\lambda_c}{\lambda_c + 2(C_B - c)t}, \tag{27}$$

where $h_{L5}(0) = D - \eta_c - \eta_t$. For the pipe diameter and flow conditions used in this paper $h_{L5}(0) \ll (D - h)$ and therefore was neglected. The liquid area $A_{L5}(t)$ is calculated from $h_{L5}(t)$ in Eq. (27) and the geometric formulae presented by Govier and Aziz (1972).

Eq. (27) provides an explanation for the behaviour of the slug length at different flow rates, which decreases when increasing the flow rates (as shown in Fig. 9). In the equation, increasing the flow rates results in larger values of, h_{L5}. This means that the rebuild rate of the liquid behind a slug increases with the flow rates, and thus the growth time of the slug decreases which results in a shorter slug.

4.2.3. Slug length, $L_S(t)$

The change in the additional liquid volume entering the slug describes the rate of change of the slug volume,

$$\frac{dV}{dt} = [C_F(t) - u_1]A_{L_{max}} - (C_B - u_5)A_{L5}(t), \tag{28}$$

and the front velocity is

$$C_F(t) = \frac{dV}{d(At)} + C_B. \tag{29}$$

To simplify the problem we assumed that C_B is constant in time.

The total slug volume is calculated from the sum of Eqs. (19) and (28),

$$V_{slug}(t) = L_0 A + \int_0^{t_\infty} ((C_F(t) - u_1)A_{Lmax} - (C_B - u_5)A_{L5}(t))dt. \tag{30}$$

Once Eq. (30) is solved, the slug length follows as

$$L_S(t) = \frac{V_{slug}(t)}{A}. \tag{31}$$

4.3. End of slug growth

If only one slug would have been initiated in the pipe, it would keep growing until it finally exits the pipe. However, in general more slugs present at the same time. A slug will stop growing as soon as its front approaches the back of the tail of the first slug downstream. Thus, we need to estimate when this happens. We do so by respecting what happens when all slugs are formed at regular distances. This means that we will find the average slug length and ignore that actually a distribution of slug lengths develops as slugs are initiated in an irregular way. However, with this approach we can estimate the average slug length and by that predict where the long slug regime is located in the flow map. As a consequence, all slugs and bubbles reach their final lengths simultaneously, say at time t_∞. This conclusion leads to a stopping criterion for the calculation of the average slug length: the final average slug length is reached when the extension of the tail (the distance between points a and b) becomes equal to the bubble final length,

$$L_{B,r}(t) = L_{B,f}, \tag{32}$$

as shown in Fig. 8. In the figure, the fully developed average slug problem is presented for a pipe cross-sectional area A. The cross-sectional liquid area of the stratified flow is $A_{L_{max}}$ and for the fully developed slug flow is $A_{L_{min}}$ along the bubble. Choosing a control volume with the unit length, $L_U = L_{B,f} + L_{S,f}$, and making a volumetric balance between the stratified flow and the fully developed slug flow cases, a relation between the bubble and slug lengths is obtained as follows:

$$L_{B,f} = L_{S,f}\frac{A - A_{L_{max}}}{A_{L_{max}} - A_{L_{min}}}. \tag{33}$$

At the limit of Eq. (33) when $A_{L_{max}} \to A_{L_{min}}$, term $L_{B,f} \to \infty$, which means that there are no slugs in the pipe, as expected.

Since $L_{S,f}, L_{B,f}, L_U$ and t_∞ are unknowns, t_∞ is calculated recursively by substituting Eqs. (18) and (32), and $L_S(t)$ instead of $L_{S,f}$, in Eq. (33) as follows:

$$t_\infty = \frac{1}{v_b}\left[L_S(t_\infty)\frac{A - A_{L_{max}}}{A_{L_{max}} - A_{L_{min}}} - L_{B,r}(t_0)\right]. \tag{34}$$

It is known from experiments (e.g. Kristiansen, 2004) that increasing the gas flow rates results in faster development of the slug flow. This is well observed in Eq. (34), at higher gas flow rates v_b increases and t_∞ decreases.

5. Results

The measurements presented in this section were performed by a number of researchers at different flow conditions and pipe sizes. A summary of the properties of the different systems is found in Table 1.

5.1. Predictions for horizontal air–water flow

Theoretical calculations of slug final lengths, $L_{S,f}$, are compared with measurements for air–water horizontal flow in Figs. 9–11. The measurements in Figs. 9 and 10 were carried out in a 137 m long pipe with 5.2 cm i.d. at the TU Delft facility (Zoeteweij, 2007). The subplots in Fig. 9 show $L_{S,f}$ as a function of U_{SG} for three different U_{SL}: 0.1032, 0.25 and 0.29 m/s. The figure shows a satisfactory agreement between predictions and measurements for the given flow rates. The vertical dashed lines indicate the critical U_{SG} for the transition from hydrodynamic to long slugs (i.e. slugs larger than 40D). The transition is further presented in Fig. 10, a flow map for different slug flow regimes and sub-regimes. Here, the dashed line represents the transition from stratified to slug

Table 1
Summary of system properties.

	Air–water	Air–water	SF_6–oil	CO_2–water
Pipe diameter (cm)	9.5, 7.63, 6, 5.2, 3.51	6	6.9	1.905
Pressure (Pa)	1×10^5	1×10^5	$1–3 \times 10^5$	1×10^5
Pipe inclination (deg)	0	−0.5	−0.1	0
Interfacial tension (N/m)	0.07	0.07	0.022	0.07
Gas density (kg/m^3)	1.2	1.2	1.2, 9, 19	1.8
Gas viscosity (kg/ms)	1.8×10^{-5}	1.8×10^{-5}	1.37×10^{-5}	1.5×10^{-5}
Liquid density (kg/m^3)	1000	1000	800	1000
Liquid viscosity (kg/ms)	0.001	0.001	0.0018	0.001

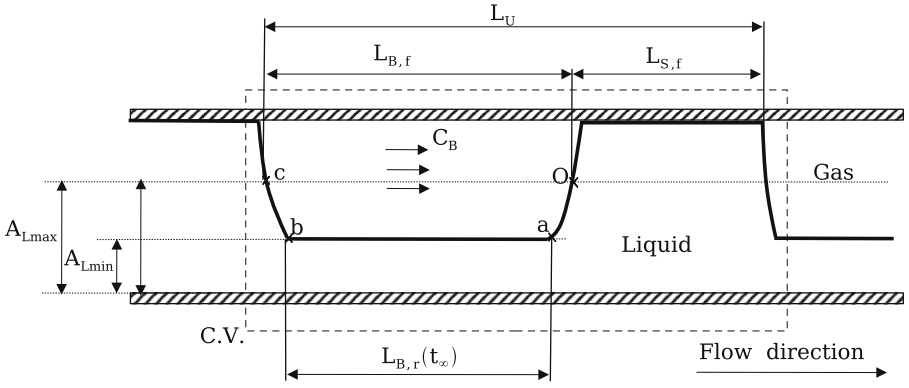

Fig. 8. A presentation of the average fully developed slug flow.

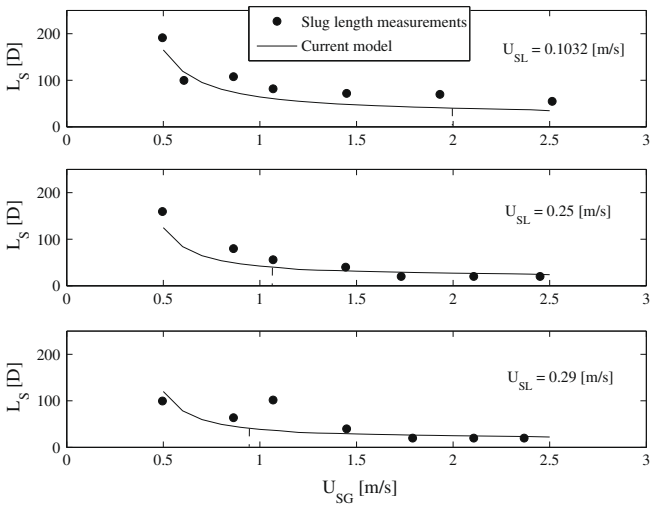

Fig. 9. Air–water theoretical predictions and measurements of slug length as a function of gas superficial velocity, $D = 5.2$ cm, $\theta = 0^\circ$, $P = 1$ bara.

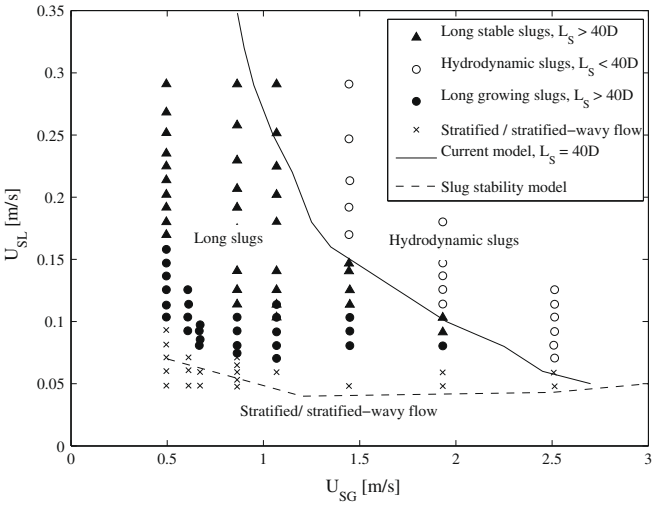

Fig. 10. Air–water theoretical predictions and measurements of the flow regime transition for different U_{SG} and U_{SL}, $D = 5.2\ cm, \theta = 0^\circ, P = 1$ bara.

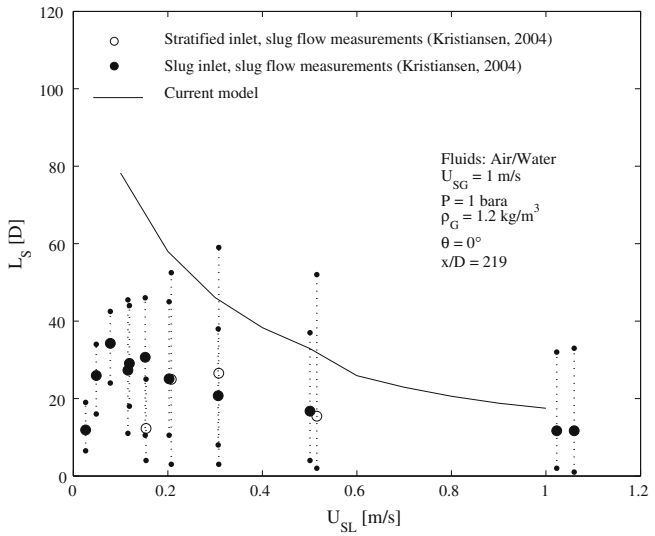

Fig. 11. Air–water theoretical predictions and measurements of slug length as a function of liquid superficial velocity, $D = 6$ cm, $\theta = 0^\circ$, $P = 1$ bara, $U_{SG} = 1$ m/s.

flow by the slug stability model, and the solid line is the prediction by the current model for $L_{S,f} = 40D$, which represents the transition from hydrodynamic to long slug regimes. The current model for the transition from hydrodynamic to long slugs underpredicts the measurement at low U_{SG}, but quite accurately predicts the transition at higher U_{SG}.

The measurements in Fig. 11 were done by Kristiansen (2004) in a 16 m pipe with i.d. of 6 cm. Two different inlet conditions were considered here, stratified and slug flow represented by empty and filled circles, respectively. The dotted vertical lines are the deviation from the average slug length. The figure shows the behaviour of the slug length as a function of U_{SL}, at $U_{SG} = 1$ m/s. It is noticeable that the theoretical model (the solid line) overpredicts the average values of the slug lengths with about a factor of 4 at low U_{SL}. A possible reason for this deviation between predictions and measurements is the short pipe length being not sufficient for developed slug flow (the slug growth rate at $x/D = 219$ is still positive, Kristiansen (2004)). Note that the inlet conditions do not have a significant impact on the slug length in the short loop.

5.2. Predictions for declined air–water flow

Figs. 12 and 13 compare theoretical predictions of the slug length with measurements, as a function of U_{SL} for $U_{SG} = 1$ and 3 m/s, respectively. The measurements were also done by Kristiansen (2004) and carried out in the same short flow loop as in Fig. 11. However, a negative inclination of -0.5° was considered here. Kristiansen (2004) found that the declination of the pipe results in lower growth rates so that slugs reach their final length earlier in the pipe, especially at lower U_{SG}. In the case of Fig. 12, where $U_{SG} = 1$ m/s, the measured slugs have reached their final length and they are in good agreement with the theoretical predictions. On the other hand, for the measurements in Fig. 13, carried out at higher U_{SG}, the pipe is too short to obtain a fully developed slug flow. Here, the model overpredicts the slug length with a factor of three at low U_{SL}, and underpredicts it with a factor of two at high U_{SL}.

5.3. Predictions for SF_6 gas–ExxsolD80 oil flow under varying pressure

The measurements shown in Figs. 14 and 15 are those performed by Kristiansen (2004) for different inlet conditions with different fluids in a longer and slightly larger facility (horizontal,

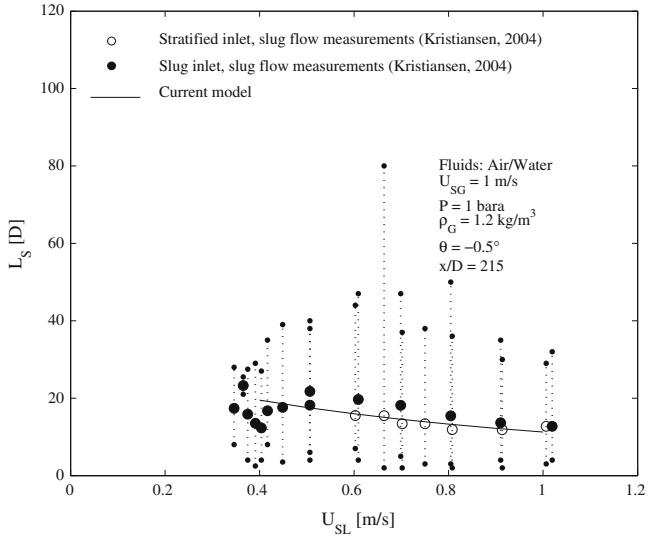

Fig. 12. Air–water theoretical predictions and measurements of slug length as a function of liquid superficial velocity, $D = 6$ cm, $\theta = -0.5^\circ$, $P = 1$ bara, $U_{SG} = 1$ m/s.

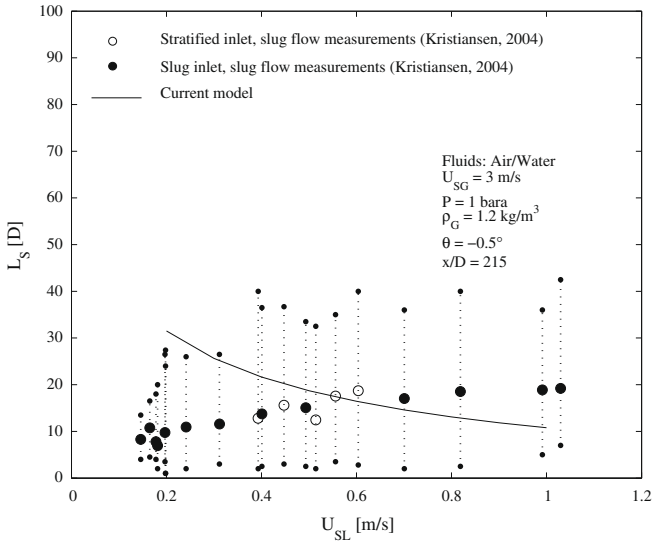

Fig. 13. Air–water theoretical predictions and measurements of slug length as a function of liquid superficial velocity, $D = 6$ cm, $\theta = -0.5^\circ$, $P = 1$ bara, $U_{SG} = 3$ m/s.

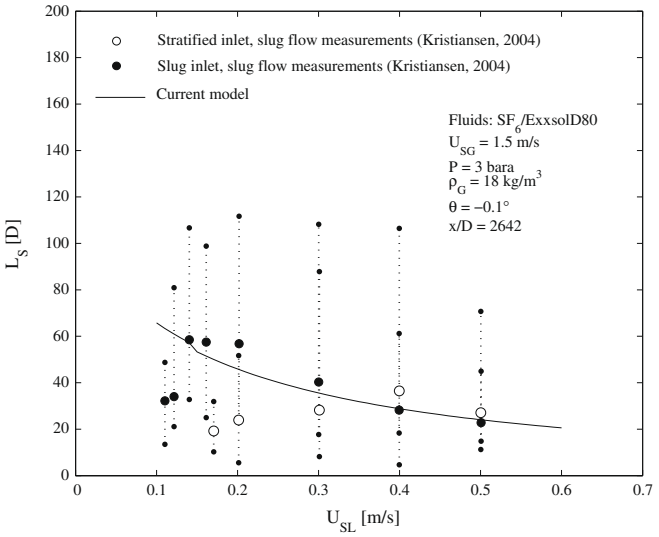

Fig. 15. SF_6–*ExxsolD*80 theoretical predictions and measurements of slug length as a function of liquid superficial velocity, $D = 6.9$ cm, $\theta = -0.1^\circ$, $P = 3$ bara, $U_{SG} = 1.5$ m/s.

103 m long test loop with an i.d. of 0.069 m). Instead of air/water he used SF_6 (sulfur hexafluoride) gas and *ExxsolD*80 (hydrocarbon fluid) liquid at two different pressures. The figures compare theoretical predictions of $L_{S,f}$ with measurements as a function of U_{SL} at constant U_{SG} and varying pressure. The predictions of $L_{S,f}$ in Fig. 14 ($P = 1.5$ bara) are in a good agreement with the slug inlet measurements. However, a deviation between the predictions and the stratified inlet measurements at $U_{SL} < 0.15$ m/2 is noticed. The reason behind the deviation is the proximity of the low U_{SL} to the pattern transition value that moves the slug initiation point further downstream in the pipe. As a result, the slugs close to the outlet are not fully developed.

At higher pressure, $P = 3$ bara, a deviation is noticed, as well, between predictions and slug inlet measurements at $U_{SL} = 0.1$ m/s (see Fig. 15). The deviation between the predictions and the stratified inlet measurements becomes even larger and for a wider range of U_{SL} ($U_{SL} < 0.4$ m/s). In the stratified inlet case, increasing the pressure results in increasing $U_{SL_{crit}}$ needed for the transition from stratified to slug flow. Therefore, the delay of the slug initiation point further downstream in the pipe corresponds, as well, to higher values of U_{SL}. That is also why in the case of $P = 3$ bara no slugs appeared for $U_{SL} < 0.17$ m/s at the given U_{SG} (the flow rates are below the critical values required for the pattern transition). In the case of the slug inlet, slugs at $U_{SL} < 0.12$ m/s are unstable (slug stability) and their growth is sensitive to small perturbations at their fronts. Therefore, they can grow or decay accordingly.

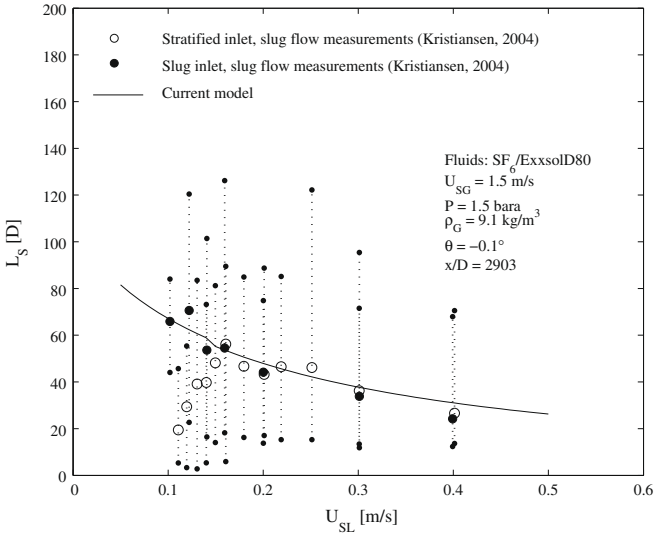

Fig. 14. SF_6–*ExxsolD*80 theoretical predictions and measurements of slug length as a function of liquid superficial velocity, $D = 6.9$ cm, $\theta = -0.1^\circ$, $P = 1.5$ bara, $U_{SG} = 1.5$ m/s.

5.4. Predictions at large mixture velocities

In this subsection we examine the effect of large mixture velocities on the predictions by the proposed model and compare the predictions to available measurements. Unfortunately, in these experiments there were no direct measurements for the slug length but for the slug frequency. For that reason, we used the following approximation, suggested by Woods and Hanratty (1996), for the relation between f_S and $L_{S,f}$ under "fully developed" conditions,

$$\frac{f_S D}{U_{SL}} = 1.2\left(\frac{L_{S,f}}{D}\right)^{-1}. \tag{35}$$

Please note that we shall denote the slug lengths derived from the slug frequency measurements via Eq. (35) in the subsequent comparisons by slug "measurements". Figs. 16 and 17 compare predictions and measurements for a 20 m length and 7.63 cm i.d. pipe. The slug frequency measurements were done by Woods and Hanratty (1999). In Fig. 16 we see that the current model overpredicts the measurements at low U_{SL}, underpredicts them at high U_{SL} and successfully predicts them at "intermediate" U_{SL}. Predictions at intermediate liquid flow rates are important for the transition from hydrodynamic to long slug flows as shown in Fig. 17, a flow map for the long (•) and hydrodynamic (○) slug measurements at different superficial flow rates. The dashed line is the slug stability line, and the solid line ($L = 40D$) represents the transition from long to hydrodynamic slugs.

Fig. 18 compares predictions with measurements in 3 different i.d. pipes: 1.905, 3.51 and 9.5 cm (in the figure from top to bottom, respectively). Each subplot shows $L_{S,f}$ as a function of U_{SG} at relatively high constant U_{SL}. The slug frequency measurements used

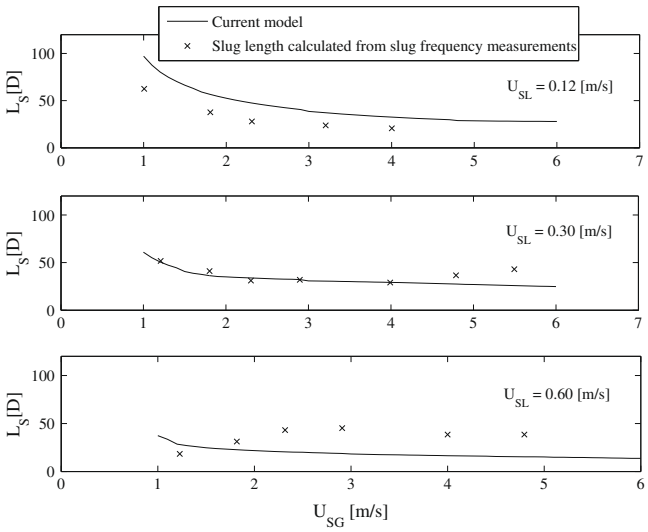

Fig. 16. Air–water theoretical predictions and measurements of slug length as a function of gas superficial velocity, $D = 7.63$ cm, $\theta = 0^\circ$, $P = 1$ bara.

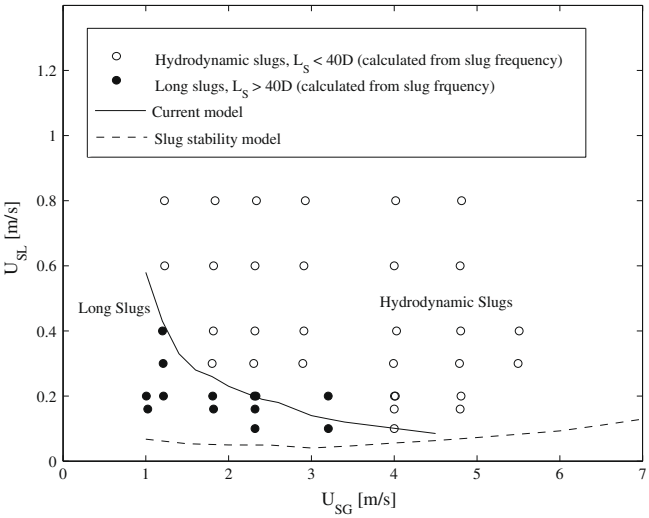

Fig. 17. Air–water theoretical predictions and measurements of the flow regime transition for different U_{SG} and U_{SL}, $D = 7.63$ cm, $\theta = 0^\circ$, $P = 1$ bara.

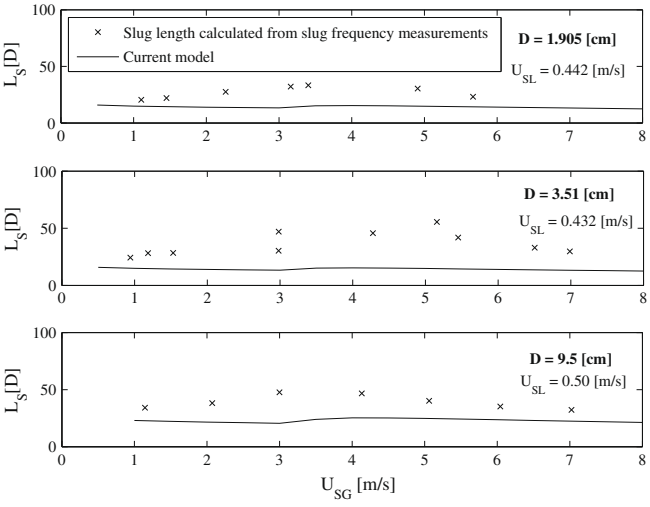

Fig. 18. Air–water theoretical predictions and measurements of slug length as a function of gas superficial velocity, $\theta = 0^\circ$, $P = 1$ bara, top subplot: $D = 1.905$ cm, middle subplot: $D = 3.51$ cm, bottom subplot: $D = 9.5$ cm.

to calculate the slug length shown in the upper subplot were done by Gregory and Scott (1969) at $U_{SL} = 0.442$ m/s; in the middle subplot by Hubbard (1965) at $U_{SL} = 0.432$ m/s; and in the bottom subplot by Fan et al. (1993) at $U_{SL} = 0.5$ m/s. The slug growth model underpredicts the measurements in all of the subplots. A possible reason for the disagreement between predictions and measurements is that the mixture velocities are not low enough to neglect the aeration, ϵ, as assumed by the model (see Eq. (13)). Considering the aeration results in lower liquid velocity in the slug, u_3, lower mixture velocity, U_{mix} (Eq. (13)), lower bubble velocity, C_B (Eqs. (8)–(10)), and therefore larger development time, t_∞ (Eq. 34) that results in larger slugs.

6. Conclusions

(1) Very long slugs, reaching 500 pipe diameter have been observed in gas–liquid horizontal pipe flow measurements. The long slugs appear at low gas flow rates, where the flow development is slow and the differences in liquid level between the front and the tail of a developing slug is large.

(2) In the long slug regime, there are two different sub-regimes: (a) stable slugs (fully developed), that have reached their final length; and (b) growing slugs. The second type appears, at critical liquid flow rates close to the transition from stratified to slug flow.

(3) At low gas flow rates the transition from stratified to hydrodynamic slug flow occurs via the long slug regime. At high gas flow rates such a long slug region does not exist and for favourable flow conditions stratified flow directly transforms into hydrodynamic slug flow.

(4) A slug growth model was presented. The growth model applies a volumetric balance between the front and the tail of a slug. In the model, the behaviour of the liquid phase at the slug tail is simplified by applying a linear kinematic relation between the back of the slug and the wave upstream. This relation is used to calculate the tail extension and the change in the liquid level. The growth model captures the main factors contributing to the slug growth behaviour. As a result, it accurately predicts the transition from hydrodynamic to long slug regimes for different pipe diameters. However, it underpredicts the average slug length at high mixture velocities. To improve the predictions, gas entrainment should be taken into consideration.

(5) The model provides an explanation for a number of important observations in the slug flow regime: (a) in the long slug regime, the slug length decreases with increasing liquid flow rates as a result of the faster development of the liquid level behind the slug (Eqs. (27) and (34)); (b) increasing the operation pressure results in larger interfacial shear stresses, lower equilibrium liquid level (Eq. (24)) and volumetric growth rate (Eq. (28)), and thus shorter average slug length – that is why at high pressure only hydrodynamic slugs are observed; (c) further increase of the pressure results in liquid levels approaching the minimum slug stability level, so that no stable slugs (long or hydrodynamic) can appear anymore (unless produced at the inlet).

(6) Our study with the long slug growth model raises important questions on: (a) the critical operation pressure and flow development time at which the long slugs appear; and (b) the contribution of the interfacial shear stresses and gas entrainment to the long slug development. Answers to these questions are key issues in reducing the negative effects of long slugs when operating at low pressure and low gas rates. These are subjects of research in progress.

Acknowledgment

This research is a part of the research project: ''Long liquid slugs in stratified gas–liquid flow in horizontal and slightly inclined tubes", sponsored by STW (Dutch Foundation for Technological Research).

References

Andritsos, N., Williams, L., Hanratty, T.J., 1989. Effect of liquid viscosity on the stratified-slug transition in horizontal pipe flow. Int. J. Multiphase Flow 15, 877–892.

Bendiksen, K.H., 1984. An experimental investigation of the motion of long bubbles in inclined tubes. Int. J. Multiphase Flow 10, 467–483.

Benjamin, T.B., 1968. Gravity currents and related phenomena. J. Fluid Mech. 31, 209–248.

Churchill, S.W., 1977. Friction-factor equation spans all fluid-flow regimes. Chem. Eng. 7, 91.

Dukler, A.E., Maron, D.M., Brauner, N., 1985. A physical model for predicting the minimum stable slug length. Chem. Eng. Sci. 40, 1379–1385.

Fan, G.W., Lusseyran, F., Hanratty, T.J., 1993. Initiation of slugs in horizontal gas–liquid flows. AIChE J. 39, 1741–1753.

Govier, G.W., Aziz, K., 1972. The Flow of Complex Mixtures in Pipes. Van Nostrand Reinhold Co., NY. p. 563.

Gregory, G.A., Scott, D.S., 1969. Correlation of liquid slug velocity and frequency in horizontal cocurrent gas–liquid slug flow. AIChE J. 15, 933–935.

Hanratty, T.J., Hershman, A., 1961. Initiation of roll waves. AIChE J. 7, 488–497.

Hubbard, M.G., 1965. An analysis of horizontal gas liquid slug flow. Ph.D. thesis, University of Houston.

Hurlburt, E.T., Hanratty, T.J., 2002. Prediction of the transition from stratified to slug and plug flow for long pipes. Int. J. Multiphase Flow 28, 707–729.

Kadri, U., Mudde, R.F., Oliemans, R.V.A., 2008. A growth model for dynamic slugs in gas/liquid horizontal pipes. In: Proc. BHR Conf., Banff, Canada, pp. 241–254.

Kristiansen, O., 2004. Experiments on the transition from stratified to slug flow in multiphase pipe flow. Ph.D. thesis, Norwegian University of Science and Technology (NTNU), Trondheim.

Lin, P.Y., Hanratty, T.J., 1986. Prediction of the initiation of slugs with linear stability theory. Int. J. Multiphase Flow 12, 79–98.

Nydal, O.J., 1991. An experimental investigation of slug flow. Ph.D. thesis, University of Oslo, Department of Mathematics, Oslo, Norway.

Ruder, Z., Hanratty, P.J., Hanratty, T.J., 1989. Necessary conditions for the existence of stable slugs. Int. J. Multiphase Flow 15, 209–226.

Soleimani, A., Hanratty, T.J., 2003. Critical liquid flows for the transition from the pseudo-slug and stratified patterns to slug flow. Int. J. Multiphase Flow 29, 51–67.

Tronconi, E., 1990. Prediction of slug frequency in horizontal two-phase slug flow. AIChE J. 36, 701–709.

Wallis, G.B., Dobbins, J.E., 1973. The onset of slugging in horizontal stratified air–water flow. Int. J. Multiphase Flow 1, 173–193.

Woods, B.D., Hanratty, T.J., 1996. Relation of slug stability to shedding rate. Int. J. Multiphase Flow 22, 809–828.

Woods, B.D., Hanratty, T.J., 1999. Influence of Froude number on physical processes determining frequency of slugging in horizontal gas–liquid flows. Int. J. Multiphase Flow 25, 1195–1223.

Wu, H.L., Pots, B.F.M., Hollenberg, J.F., Meerhoff, R., 1987. Flow pattern transitions in two-phase gas/condensate flow at high pressure in an 8-inch horizontal pipe. In: Proc. BHRA Conf., The Hague, The Netherlands, pp. 13–21.

Zoeteweij, M.L., 2007. Long liquid slugs in horizontal tubes. Development study and characterisation with electrical conductance techniques. Ph.D. thesis, Delft University of Technology, Department of Multi-Scale Physics, Delft, The Netherlands.